Journal of Alloys and Compounds 503 (2010) 281–285

Contents lists available at ScienceDirect

Journal of Alloys and Compounds

journal homepage: www.elsevier.com/locate/jallcom

The crystal structure of La-doped $Co_{40}V_{60}$ compound

X.J. Chen [a,b], H.Y. Zhou [a,*], T. Wang [b], Y.Q. Yang [b], G.H. Rao [b]

[a] Department of Information Materials Science and Engineering, Guilin University of Electronic Technology, Guilin, Guangxi 541004, PR China
[b] Beijing National Laboratory for Condensed Matter Physics, Institute of Physics, Chinese Academy of Sciences, Beijing 100190, PR China

ARTICLE INFO

Article history:
Received 5 January 2010
Received in revised form 6 April 2010
Accepted 7 April 2010
Available online 14 April 2010

Keywords:
σ phase
Rare earth metal incorporation
Stability and crystal structure
X-ray diffraction

ABSTRACT

Crystal structure of the compounds $Co_{40}V_{60-2x}La_x$ has been investigated by means of X-ray powder diffraction (XRD). The compounds crystallize in the tetragonal σ phase structure with the space group $P4_2/mnm$ and form a solid solution with a solubility limit of $x = 9.52$. The lattice parameters a, c and the unit cell volume V of the compounds decrease linearly with the La content. A structure model with a preferential substitution of La for V atoms on the 8j sites accompanied by the presence of vacancies on these sites is proposed for $Co_{40}V_{44}La_8$. The proposal structure model gives a satisfactory fitting to the XRD data and a reasonable La content close to the nominal composition as well as a coincidence of the calculated density with the experimentally measured one. The preferential occupation of La atoms on the 8j site is discussed based on a consideration of geometric constrain and thermodynamics.

1. Introduction

Nowadays, the σ phase is known to exist in 43 binary alloy systems. It was discovered in 1923 in Fe–Cr alloy and has been extensively studied regarding to its stability, crystal structure, distribution of atoms, order–disorder transformation, mechanical and physical properties [1]. The σ phase belongs to the group of the Frank–Kasper compounds (topologically close-packed phases). Its unit cell contains 30 atoms distributing among five crystallographically non-equivalent sites: 2a, 4f, $8i_1$, $8i_2$, and 8j, of the space group $P4_2/mnm$ [2]. Stuwe has shown that the σ phase can be viewed as a sphere-packing structure [3]. The contents of a unit cell of the σ phase structure can be described as consisting of interlocking hexagonal rings of A, B, C and D-type atoms surrounding four pairs of E-type atoms situated at $z = 1/4$ and $z = 3/4$ (A, B, C, D and, E denoted atoms on the 2a, 4f, $8i_1$, $8i_2$ and 8j sites, see Fig. 1). On the horizontal layers, atoms on the A, B, C and D sites construct a quasi-hexagonal symmetry about the vertical rows of E-type atoms. The E-type atoms have the effect of contracting the size of the pseudo-hexagonal rings. The rows of E-type atoms threading the close-packed layers appear to bind the two layers together. In addition, the σ phase structure is analogous to the Zr_4Al_3 structure [4]. In the σ phase structure the two layers of atoms having pseudo-hexagonal symmetry correspond to the layers of alternate Zr and Al atoms in the Zr_4Al_3 structure. The difference between them is that the pseudo-hexagonal layers in Zr_4Al_3 structure are symmetrical about the common hexagonal axis, while the corresponding layers in σ phase have their hexagonal axes displaced relative to each other (see projection of the structures along the c-axis, Fig. 2). Although the layered structure and stacking of the σ phase are similar to those of the Zr_4Al_3 (space group $P6/mmm$), the departure from hexagonal symmetry leads to an inexact placing of the atoms of one layer above the hollows of the layer below. This imperfect form of stacking has a merit of providing a flexibility in the ratio of X:Y atoms that can be accommodated in each layer and hence the wide range of composition is generally found in binary σ phase.

Both the Zr_4Al_3 structure and the σ phase structure are closely related to the $CaCu_5$-type structure (space group $P6/mmm$), the primary structure of various R-T intermetallic compounds (R and T stand for rare earth metal and transition metal, respectively). The Zr_4Al_3 structure can be viewed as a derivative of the $CaCu_5$-type structure in which all the Ca atoms, which lie along the hexagonal axes of the simple kagomè net at $z = 0$, are replaced by Zr atoms at $z = 1/4$ and $z = 3/4$, forming Zr–Zr dumbbells [5]. Many other types of structures, such as $TbCu_7$, Th_2Zn_{17}, $ThMn_{12}$, $Nd_3(Fe,Ti)_{29}$, etc., can be derived from the $CaCu_5$-type structure by using transition metal dumbbells T-T to substitute part of large rare earth atoms R on the Ca sites in an appropriate ordered or disordered way [6,7]. Fig. 2 shows the projections along the c-axis of the $CaCu_5$, Zr_4Al_3 and the σ phase structures.

Inspired by the discovery and excellent permanent magnetic properties of $SmCo_5$ and $Nd_2Fe_{14}B$ intermetallics, extensive exploration of novel rare earth permanent magnets in rare earth-transition metal systems has been implemented, and as a consequence many rare earth-transition metal intermetallics

* Corresponding author.
E-mail addresses: zhy@guet.edu.cn (H.Y. Zhou), ghrao@aphy.iphy.ac.cn (G.H. Rao).

0925-8388/$ – see front matter © 2010 Elsevier B.V. All rights reserved.
doi:10.1016/j.jallcom.2010.04.045

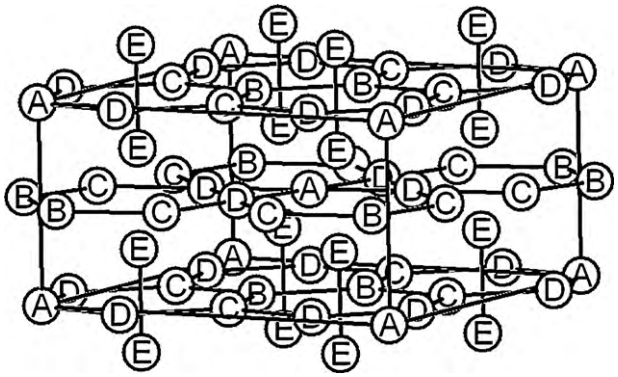

Fig. 1. Crystal structure of σ phase. A, B, C, D and E correspond to the 2a, 4f, $8i_1$, $8i_2$ and 8j atomic positions.

with the $CaCu_5$ derivative structures and promising permanent magnetic properties have been fabricated. Among these $CaCu_5$ derivative structures, the highest transition metal content occurs in the $R(Fe,M)_{12}$ with the $ThMn_{12}$-type structure, in which half of the R atoms in the $CaCu_5$ structure were substituted by the transition metal dumbbells in an ordered way. As discussed above, the σ phase structure is analogous to the $CaCu_5$ derivative structure with all the Ca atoms being substituted by dumbbell atoms. It would be anticipated that rare earth-transition metal intermetallic compounds with the $CaCu_5$ derivative structure and the transition metal content higher than that in $R(Fe,M)_{12}$ might be achieved if some pairs of the E atoms in the σ phase could be substituted by R atoms in an ordered way, accompanied by an appropriate modification of the structure.

It is well known that the σ phase is a hard brittle phase present in a lot of technologically important systems. Therefore, extensive studies have been performed on the σ phase-related systems mostly to avoid the appearance of the σ phase. However, the solubility of rare earth atoms in the σ phase and its influence on the structure as well as the distribution of rare earth atoms has been scarcely reported. In this work, we prepared $Co_{40}V_{60-2x}La_x$ compounds, nominally assuming that one La atom substitutes for a pair of transition metals in $Co_{40}V_{60}$ σ phase, and determined the crystal structure of the compounds and the occupation of the La atoms in the structure by means of X-ray powder diffraction.

2. Experiment

Polycrystalline alloy samples of $Co_{40}V_{60-2x}La_x$ were prepared by arc melting appropriate amounts of pure metals V, Co and La under high-purity Ar atmosphere. An excess amount of La was added to compensate for the loss during melting and annealing. All the ingots were remelted several times to ensure homogeneity. The obtained ingots were wrapped in tantalum foil, sealed into evacuated quartz tubes, annealed at 1173 K for 2 weeks, and then quenched in water. The samples were ground into powder for X-ray powder diffraction (XRD) experiments. The XRD data were collected on a Rigaku D/max-2500 diffractometer with Cu Kα radiation (45 kV × 250 mA) and a graphite monochromator. XRD data used for structural analysis were recorded by a step scan mode with a step width of $2\theta = 0.02^\circ$ and a sampling time of 2 s in the range of $20^\circ \le 2\theta \le 120^\circ$.

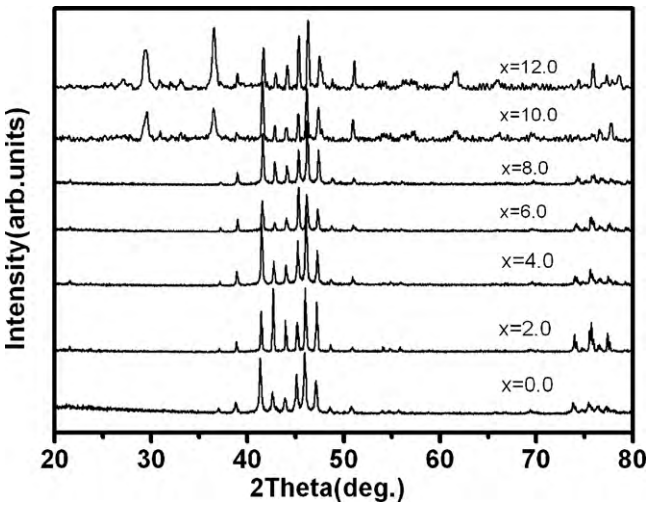

Fig. 3. Powder XRD patterns of $V_{60-2x}La_xCo_{40}$ alloys.

3. Results and discussion

3.1. Solid solubility

Fig. 3 shows the XRD patterns of the alloys $Co_{40}V_{60-2x}La_x$ with different La contents from $x = 0$ to $x = 12.0$. According to indexing and profile fitting results, the XRD patterns show that the samples of $V_{60-2x}La_xCo_{40}$ with $0.0 \le x \le 8$ crystallize in the σ phase with the space group $P4_2/mnm$, whereas the $V_{60-2x}La_xCo_{40}$ with $x = 10.0$ and 12.0 are composed of La_4Co_3 phase and the σ phase. Fig. 4 shows the dependence of the lattice parameters a and c as well as the unit cell volume V of the σ phase on the La content in the $Co_{40}V_{60-2x}La_x$ compound. The nearly linear dependence of the lattice constants on the concentration indicates that the samples form a single phase solid solution. Suppose the solid solution is a substitutional one without introducing vacancies and with La taking the place of larger V atoms in the V–Co σ phase, then the lattice constants of $Co_{40}V_{60-2x}La_x$ should be larger than those of corresponding $Co_{40}V_{60-x}$, which is inconsistent with the observations. The lattice parameters a, c

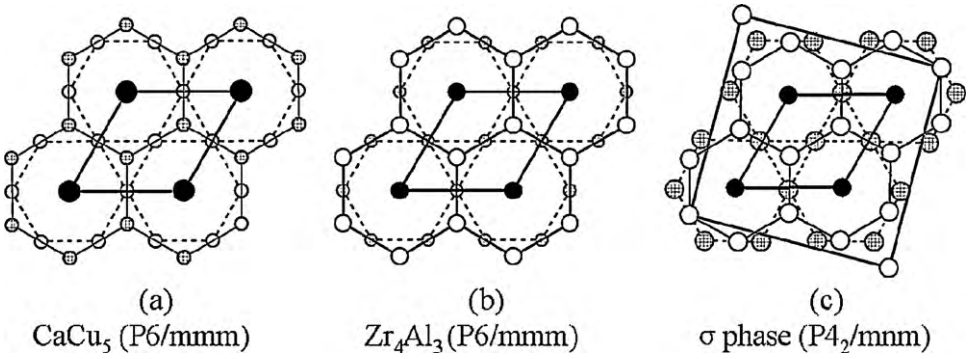

Fig. 2. Projections of the structures of $CaCu_5$, Zr_4Al_3 and σ phase along the c axis.

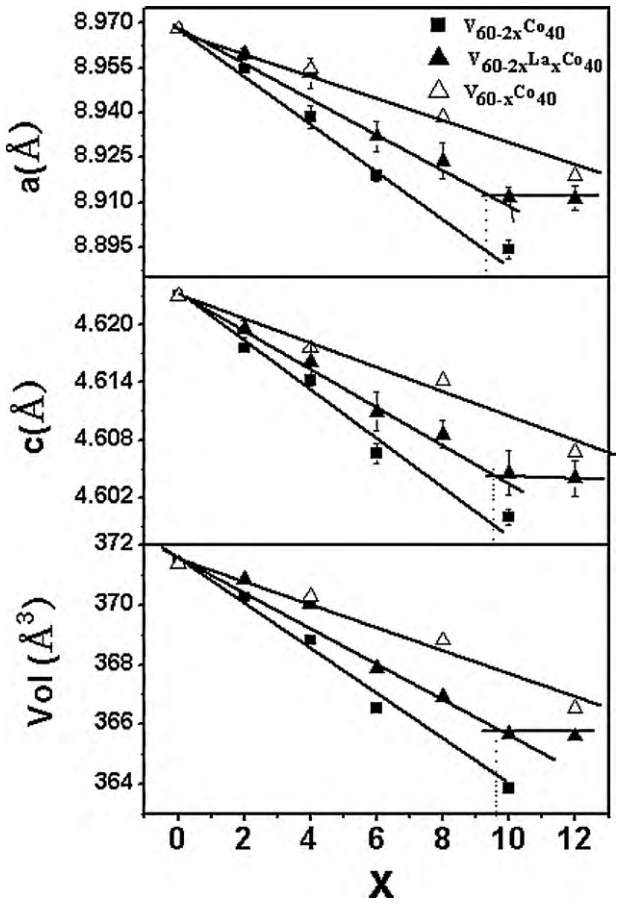

Fig. 4. Evolution of the lattice parameters and the cell volume of $V_{60-2x}La_xCo_{40}$ (triangles). For comparison, the lattice parameters of $Co_{40}V_{60-x}$ (follow triangle) and $Co_{40}V_{60-2x}$ (circles) are also plotted.

and cell volume *V* are larger than those of the corresponding Co–V binary alloy with the same Co/V ratio, i.e., $Co_{40}V_{60-2x}$, manifesting the incorporation of the La atoms possibly into interstitial sites or a consequence of atom redistribution in the σ phase structure. Though the distribution of the d-electron-poor and the d-electron-rich metals is generally not random in the σ phase, the structural data of various σ phase compounds collected by Joubert [8] exhibits an almost linear composition dependence of lattice parameters as evidence in Fig. 4 for $Co_{40}V_{60-x}$ and $Co_{40}V_{60-2x}$. Therefore, it is reasonable to estimate the solubility limit of the σ phase solid solution as the compositions where kinks take place on the lattice parameter versus composition curve, according to the Gibbs' phase rule. Based on the variation of the lattice parameter with the concentration of the substituting element, the maximum solid solubility of La in $V_{60-2x}La_xCo_{40}$ σ phase is determined to be about $x = 9.52$, i.e. 10.5 at.%.

3.2. Structure refinement

The crystal structure of the $V_{60-2x}La_xCo_{40}$ compounds was refined by Rietveld method based on the σ phase structure, using the program Rietan 2000 [9]. The $Co_{40}V_{60}$ compound crystallized in the σ phase with the space group $P4_2/mnm$ [10]. We adopted the σ phase structure of the $Co_{40}V_{60}$ as the initial structure to refine the XRD data of $Co_{40}V_{60-2x}La_x$. The Legendre polynomial function was fitted to background intensity with twelve adjustable parameters. The split pseudo-Voigt function was used to fit the peak profile. All the refinable atomic coordinates were varied independently along with the unit-cell parameters. The sample displacement was refined to correct the zero shift of the X-ray diffraction pattern. The overall isotropic atomic displacement parameter B was refined. The sample absorption correction was not taken into account since the planar specimen was used.

For the binary σ phase, the actual distribution of constituent elements has been extensively studied by various techniques [8]. The site occupation parameters were found to vary with composition and annealing temperature, causing a variation in the average near neighbor environment of different sites. In general, larger atoms such as V prefer the sites with high CN (coordination number), i.e. 4f (CN = 15), $8i_1$ (CN = 14) and 8j (CN = 14) sites. These sites have more space to accommodate larger atoms and are closer to the atomic environment in the bcc structure. On the contrary, there is a clear tendency for the smaller Co atom to be accommodated in the site with low CN, i.e. 2a and $8i_2$ sites with CN = 12, leading to a similar environment of the Co in hcp structure. Since the difference in X-ray scattering power between Co and V is small, it is difficult, if not impossible, to refine site occupancies of Co and V simultaneously with a single set of XRD data. In addition, it is also difficult to refine respective occupancies of more than two species on the same crystallographic position with a single set of diffraction data. Therefore, in refinement of crystal structure of $Co_{40}V_{60-2x}La_x$, the occupancies of each constitutes on different sites in the initial model were referred to those of V-rich σ phases collected by Joubert [8] with V content of ~60 at.%. Three kinds of initial structure models were considered. The crystal structure of $Co_{40}V_{44}La_8$, which contains the highest La content among the investigated compounds, was refined in detail to highlight the distribution of rare earth atoms in the structure.

The first model is basically a substitutional one, assuming absence of any vacancy in the structure and a partial substitution of La for V on larger sites, i.e. 4f, $8i_1$ and 8j, one by one or simultaneously, since La is the largest among the three constitutes La, V, and Co. The occupancies of La were refined while the occupancies of Co were fixed to those of Fe in $V_{60}Fe_{40}$ collected in Ref. [8]. The second model is the so-called dumbbell model, i.e. a La atom substitutes a pair of V atoms on 8j site as described in Section 1. Then the La would occupy $4f_2$ site $(x, x, 0)$ with $x \sim 0.18$ or 4g site $(x, -x, 0)$ with $x \sim 0.32$ or both the $4f_2$ and 4g sites. The occupancies of La were refined, while the occupancy of V on 8j site varies accordingly as in $TbCu_7$ structure [11] and the occupancies of Co were fixed to those of Fe in $V_{60}Fe_{40}$ collected in Ref. [8]. In the third kind of model, existence of vacancies is allowed on larger sites (4f, $8i_1$ and 8j) where La atoms substitute part of V atoms wherein.

Refinements of the XRD data with the first two kinds of structural models resulted in high weighted residual pattern factor R_{wp} values (>13%) or unreasonable negative occupancies of atoms. With the third kind of structural model, the refinements were improved ($R_{wp} \sim 10\%$) saliently and strongly indicated a preferential occupation of La on the 8j site.

The final proposed structure model for $V_{44}Co_{40}La_8$ is therefore the third kind with the 8j sites being occupied by Co, V, La and some vacancy. As mentioned above, it is difficult to distinguish Co atoms from V atoms by XRD, we assumed that, for simplicity, the smaller 2a and $8i_2$ sites were exclusively occupied by Co atoms, while the larger 4f and $8i_1$ sites by V atoms. Since no impurity phase was detected according to the structure-free profile matching result, we fixed the Co/V ratio to be 40/44 as nominal composition, while the La occupancy on the 8j site was refined along with other atomic parameters and profile parameters. Then the occupancies of Co and V atoms on the 8j site were constrained by the equation: O(V) = 1.1*O(Co)-0.125 (O denotes occupancy). Nevertheless, the occupancy of Co (or V) and that of La on the 8j site still showed strong correlation during the refinement. By adjusting the occupancy of Co, Co(8j), on the 8j site, the R_{wp} showed a minimum value of 9.35% at Co(8j) = 0.21 (Fig. 5), which is supposed to

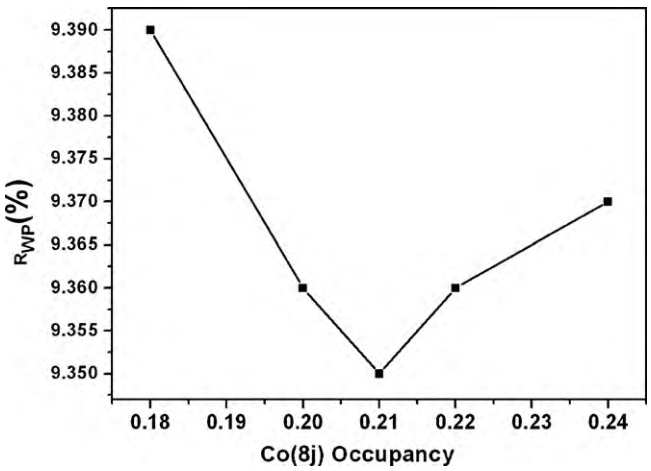

Fig. 5. The variation of R_{wp} on occupancy of Co atoms on the 8j site.

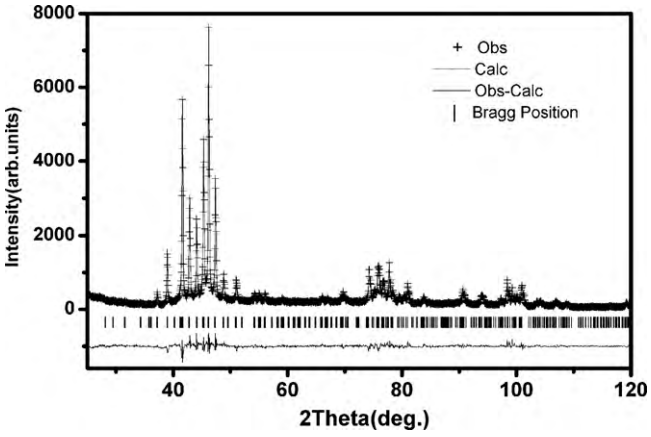

Fig. 6. XRD patterns of $Co_{40}V_{44}La_8$. The calculated and experimental patterns are represented by crosses and solid line, respectively. The bottom curve is the difference between the experimental and the calculated patterns. The vertical bars denote the position of diffraction peaks of the σ phase.

be the most probable occupancy for the Co atoms on the 8j site. Fixing Co(8j) = 0.21, the final refinement results for $Co_{40}V_{44}La_8$ is shown in Fig. 6 and the atomic parameters are listed in Table 1. The calculated and experimental patterns are represented by crosses and solid line, respectively. The bottom curve is the difference between the experimental and the calculated patterns. The vertical bars denote the position of diffraction peaks of the σ phase. The agreement of the theoretical pattern with the experimental is satisfactory. The refined lattice parameters of $Co_{40}V_{44}La_8$ are: a = 8.9246(2) Å and c = 4.6076(1) Å. The residual pattern factor R_p and the weighted residual pattern factor R_{wp} are 7.36% and 9.35%, respectively. The overall isotropic atomic displacement parameter is 0.68(2) Å^2. The refinement results give the composition of the compound as $Co_{40}V_{44}La_{7.53(5)}$, in good agreement with the nominal composition. Some typical atomic distances in $Co_{40}V_{44}La_8$ are listed in Table 2. The average atomic distances on the 2a, 4f, $8i_1$, $8i_2$ and 8j sites are 2.541, 2.744, 2.683, 2.556 and 2.681 Å, respectively, in correct order corresponding to the coordination numbers of the sites. In addition, the expected density of 7.46 g/cm^3 based on the refinement results agrees well with the experimental density of 7.40 g/cm^3 measured after Archimedes principle, further justifying the refinement results.

We also attempted to include some La atoms on the $4f_2$ and 4g sites, i.e. partial substitution of a La atom for a pair of V atoms on the 8j site, into the proposed structure model, but the refined occupancies on the $4f_2$ and 4g sites were very small and less than 5% of total La atoms were found on the $4f_2$ and 4g sites. Therefore, the present XRD data prevented us from reaching a conclusive results pertaining to this kind of inverse dumbbell substitution.

The preferential occupation of La atoms on the 8j site in $Co_{40}V_{44}La_8$ might be understood by taking into account the geometric constrain and thermodynamics. On the one hand, La is the largest in size among La, V and Co, and it should favor the atomic sites of high CN, i.e. 4f, $8i_1$ and 8j sites. On the other hand, the formation enthalpy between La and V atoms is positive and the largest among all the La-3d metal systems, while the formation enthalpy between La and Co atoms is negative [12], so La would favor positions with more Co as nearest neighbors. Then, it seems that the 4f

Table 1
Atomic parameters for the compound $Co_{40}V_{44}La_8$ derived from Rietveld refinement (R_p = 7.36%, R_{wp} = 9.35%, R_I = 7.13%, R_F = 5.98%, $S = R_{wp}/R_e$ = 1.67).

Atom	Site	x	y	z	Occupancy
Co	2a	0	0	0	1.0
Co	$8i_2$	0.7408(3)	0.0670(3)	0	1.0
Co	8j	0.1819(8)	0.1819(8)	0.252(2)	0.21
V	4f	0.3943(4)	0.3943(4)	0	1.0
V	$8i_1$	0.4666(2)	0.1265(3)	0	1.0
V	8j	0.1819(8)	0.1819(8)	0.252(2)	0.106
La	8j	0.1819(8)	0.1819(8)	0.252(2)	0.275(2)

Table 2
Selected interatomic distances in $Co_{40}V_{44}La_8$ (M = 0.21Co + 0.106V + 0.275La).

Atom		Distance/Å
Co2a		
$Co8i_2$	×4	2.389(3)
M8j	×4	2.573(8)
V4f	×4	2.662(2)
V4f		
$V8i_1$	×2	2.476(4)
Co2a	×2	2.662(2)
V4f	×1	2.668(5)
$Co8i_2$	×4	2.703(2)
M8j	×4	2.891(8)
M8j	×2	2.921(8)
$Co8i_2$		
Co2a	×1	2.389(3)
$Co8i_2$	×1	2.426(4)
$V8i_1$	×1	2.504(3)
$V8i_1$	×1	2.532(4)
$V8i_1$	×2	2.537(1)
M8j	×2	2.570(8)
M8j	×2	2.600(8)
V4f	×2	2.703(2)
$V8i_1$		
$V8i_1$	×1	2.335(4)
V4f	×1	2.476(4)
$Co8i_2$	×1	2.504(3)
$Co8i_2$	×1	2.532(4)
$Co8i_2$	×2	2.537(2)
M8j	×2	2.815(8)
$V8i_1$	×4	2.835(2)
M8j	×2	2.837(8)
M8j		
M8j	×1	2.285(1)
M8j	×1	2.322(13)
$Co8i_2$	×2	2.570(8)
Co2a	×1	2.573(8)
$Co8i_2$	×2	2.600(8)
$V8i_1$	×2	2.815(8)
$V8i_1$	×2	2.837(8)
V4f	×2	2.891(8)
V4f	×1	2.921(8)

position with CN = 15 and six neighboring Co atoms should be the preferential position for La atoms. However, the shortest distance between atoms occurs on the 8j position and the distance between La and Co atoms is much smaller on the 8j site than on the 4f site, so the La–Co interaction on the 8j site is stronger than that on the 4f site, noting that the number of coordinated Co atoms on the 4f is only one more than that on the 8j sites (6 and 5, respectively) in an ordered σ phase A_2B.

The proposal structural model for $Co_{40}V_{44}La_8$ gives a satisfactory fitting to the XRD data and a reasonable La content close to the nominal composition as well as a coincidence of the calculated density with the experimentally measured one, nevertheless, it is desirable to have multiple sets of XRD data or a combination of XRD and NPD data to accurately determine the distribution of the atoms in ternary σ phase, in particular to discern V and Co atoms as well as the occupancies of three atoms on the same equivalent crystallographic position.

4. Conclusion

The single phase alloys $Co_{40}V_{60-2x}La_x$ were synthesized. The alloys form a solid solution of the tetragonal σ phase structure (space group $P4_2/mnm$) with a solubility limit of $x = 9.52$, based on XRD results. The lattice parameters a, c and the unit cell volume of the solid solution decrease with the La content, indicating the incorporation of La in the σ phase. A structure model with a preferential substitution of La for V atoms and presence of vacancies on the 8j site is proposed for $Co_{40}V_{44}La_8$. The proposal structure model gives a satisfactory fitting to the XRD data and a reasonable La content close to the nominal composition as well as a coincidence of the calculated density with the experimentally measured one. The preferential occupation of La atoms on the 8j site could be readily understood by taking into account the geometric constrain and thermodynamics.

Acknowledgements

This work was supported by the National Natural Science Foundation of China (Grant No. 50631040) and Ministry of Science and Technology of China (Grant No. 2006CB601101).

References

[1] E.C. Bain, Chem. Met. Eng. 28 (1923) 23.
[2] G. Bergmann, D.P. Shoemaker, Acta Cryst. 7 (1954) 857.
[3] H.P. Stuwe, Trans. Met. Soc. AIME 215 (1959) 408.
[4] C.G. Kasper, D.K. Thomas, Acta Cryst. 13 (1960) 56.
[5] F.C. Frank, J.S. Kasper, Acta Cryst. 12 (1959) 483.
[6] H.H. Stadelmaier, Z. Metallkde. 75 (1984) 227.
[7] J.K. Liang, X.L. Chen, Q.L. Liu, G.H. Rao, Prog. Nat. Sci. 12 (2002) 1.
[8] J.M. Joubert, Prog. Mater. Sci. 53 (2008) 528.
[9] F. Izumi, T. Ikeda, Mater. Sci. Forum 321–324 (2000) 198.
[10] E.O. Hall, S.H. Algie, Metall. Rev. 94 (1966) 61.
[11] K.H.J. Buschow, A.S. VanderGo, Acta Cryst. B27 (1971) 1085.
[12] G.H. Rao, S. Wu, X.H. Yan, Y.L. Zhang, W.H. Tan, J.K. Liang, J. Alloys Compd. 202 (1993) 101.